Urol Res (2009) 37:253–256
DOI 10.1007/s00240-009-0204-6

CASE REPORT

Spectral diagnosis and analysis of a superior vesical artery calcification

Ted Hueih-Shing Hsu · Shan-Yang Lin · Chih-Cheng Lin · Wen-Ting Cheng · Mei-Jane Li

Received: 22 May 2009 / Accepted: 27 May 2009 / Published online: 16 June 2009

Abstract A case of urinary vessel calcification was detected incidentally in pelvic cavity of a 59-year-old man by computed tomography. The silver reticulin, actin, and hematoxylin and eosin stains were applied to diagnose the feature of vessel and confirmed that the vessel was the vesical artery. To our knowledge, this is the first report to find out the obliteration of superior vesical artery caused by calcified deposit. The calcified deposit in superior vesical artery was qualitatively identified to consist of hydroxyapatite, cholesterol and β-carotene by Fourier transform infrared and Raman microspectroscopies, in which A-type carbonated apatite was a predominate component.

Keywords Urinary vessel calcification · CT · Histopathological stain · FT-IR/Raman · Hydroxyapatite · Cholesterol · β-Carotene

Introduction

From the anatomy of vesical artery, the bladder can receive its blood supply from the superior, middle, and inferior vesical arteries. The superior vesical artery supplies the dome of the bladder, and one of its branches gives off the artery to the ductus deferens in males. It has been reported that unilateral ischemia was apparently created by ligation of either vesical artery that supply the bladder [1]. If the obliteration caused by calcified deposit is occurred in the superior or inferior vesical artery, it may obstruct the blood supply to the bladder, leading to the dysfunction of bladder.

The vibrational spectroscopy has been extensively used with a great potential over other diagnostic techniques to successfully investigate the chemical composition of the diseased tissue, rather than histological pathology alone [2, 3]. Fourier transform infrared (FT-IR) and Raman spectroscopies provide similar but complementary information on molecular–structural fingerprints of the samples. Both techniques are suitable for analyzing mineral structure with fast and nondestructive analysis since they are also sensitive to the changes in crystallinity or molecular substitution [4, 5]. These spectrophotometers were equipped with a microscopy to further provide a nondestructive method for probing biological micro-samples without further sample preparation. Several human calcified tissues such as calcinosis cutis, skin pilomatrixoma, cornea, senile cataractous lens, vitreous asteroid bodies, and sclera had been investigated by using these vibrational microspectroscopic techniques [6, 7].

Herein, we first report the case of a man with a calcification within a superior vesical artery. The calcified deposit was isolated and analyzed by Fourier transform infrared (FT-IR) and Raman microspectroscopies.

Materials and methods

Patient

A 59-year-old male patient with final stage of renal disease on hemodialysis for 11 years presented with gross

T. H.-S. Hsu
Division of Urology, Department of Surgery,
Lotung Pohai Hospital, Lotung, Ilan, Taiwan

S.-Y. Lin (✉) · C.-C. Lin · W.-T. Cheng
Department of Biotechnology, Yuanpei University,
Hsin-Chu, Taiwan, ROC
e-mail: sylin@mail.ypu.edu.tw

M.-J. Li
Department of Medical Research and Education,
Taipei Veterans General Hospital, Taipei, Taiwan, ROC

hematuria. Positive of malignant cells in urinary cytology was found, due to a papillary tumor on the dome of the urinary bladder inspected by ultrasonic cystofiberscopy. He received a transurethral resection of bladder tumor and treated intravesical chemotherapy with BCG (bacillus Calmette–Guerin) 81 mg once per week for six courses. However, in the follow-up, the cystoscopy still found a papillary growth in bladder. Under the impression of tumor recurrent, he decided to take the bladder out. The patient was explained very clearly about surgery and signed the consent form before the procedure. Radical cystoprostatectomy and bilateral nephroureterectomy were also performed. Postoperative course was uneventful. A calcific density was observed in pelvic cavity by using a computed tomography. The micro-sized calcified deposit was isolated and sent for the histopathological examination and spectral analysis. This study was approved by the Institutional Review Board at the Lotung Pohai Hospital according to the declaration of Helsinki.

Materials

Hydroxyapatite (>100 mesh, purity >99.5%), β-carotene and cholesterol as a standard reference were purchased from Nacalai Tesque, Inc. (Tokyo, Japan) and were used without further purification.

Histopathological examination

In order to verify the occurrence of calcification in which type of vessel, the isolated sample in part was formalin fixed, paraffin embedded, and investigated by means of histopathological examination. The silver reticulin, actin and hematoxylin and eosin (H&E) stains were carried out. The sample was observed by using the light microscopy (BH-2, Olympus, Tokyo, Japan).

Vibrational microspectroscopic study

The sample of calcified deposit was washed with distilled water for two times and centrifuged. The sample was then dried for 1 day at 25°C, 50% RH conditions. The dried samples were directly examined to identify and to determine the chemical component by using both Fourier transform infrared (FT-IR) microspectroscopy (Micro FTIR-200, Jasco Co., Tokyo, Japan) with a transmission technique and confocal micro-Raman spectrophotometer (Ventuno, Jasco Co., Tokyo, Japan) equipped with a 30 mW green (532 nm) solid-state laser via nondestructive analysis [6, 7]. The IR spectra were carried out at 200 scans and a resolution of 4 cm^{-1}, but the pixel resolution of Raman system was 1.3 cm^{-1}.

Spectral data acquisition and handling

Spectral analysis

A spectra manager (Jasco Co., Tokyo, Japan) and GRAMS spectroscopy software suite (Thermo Electron Co., MA, USA) were used for spectral data processing. Second-derivative FT-IR spectral analysis was applied to locate the position of the overlapping components of samples.

Compositional component determined by curve-fitting program

The chemical composition of calcified deposit in vesical artery was qualitatively and quantitatively examined by Fourier transform infrared (FT-IR) and Raman microspectroscopies [6–8]. The IR spectral ranges within 888 and 862 cm^{-1} were quantitatively estimated by the curve-fitting algorithm using the Gaussian function with the minimum standard error. The chemical composition of calcified deposit in vesical artery was computed to be the fractional area of the corresponding peak, divided by the sum of the areas of all the peaks.

Results and discussion

A calcific density was easily observed in pelvic cavity by using a computed tomography, as shown in Fig. 1A. From the histopathological results, a silver reticulin stain for differentiation of arterioles (Fig. 1B), an actin stain for smooth muscle cells in vessel walls (Fig. 1C) and a hematoxylin and eosin (H&E) stain for calcified deposit (Fig. 1D) were, respectively, evidenced. This clearly confirms that the vessel of calcified deposit was to be the vesical artery.

The FT-IR and Raman spectra of calcified deposit, cholesterol, hydroxyapatite (HA) and β-carotene are displayed in Fig. 2. Obviously, the FT-IR spectrum of calcified deposit was very close to that of the FT-IR spectrum of HA in the spectral range from 800 to 1,200 cm^{-1} (Fig. 2A). A broad absorption shoulder at 873 cm^{-1} due to bending vibration of the carbonate ion and several sharp peaks at 961, 1,031, and 1,090 cm^{-1} corresponding to the v_1 and v_3 stretching modes of phosphate were presented in both IR spectra. This suggests that HA should be the predominant component of the calcified deposit. Moreover, the IR peak at 1,467 cm^{-1} for calcified deposit was near to that of IR peak at 1,465 cm^{-1} for cholesterol, implying that cholesterol might be also contained in the calcified deposit.

The Raman spectrum of calcified deposit was more clearly manifested by the presence of cholesterol and β-carotene, except the presence of HA (Fig. 2B). A unique peak at 962 cm^{-1} was found in the Raman spectrum of

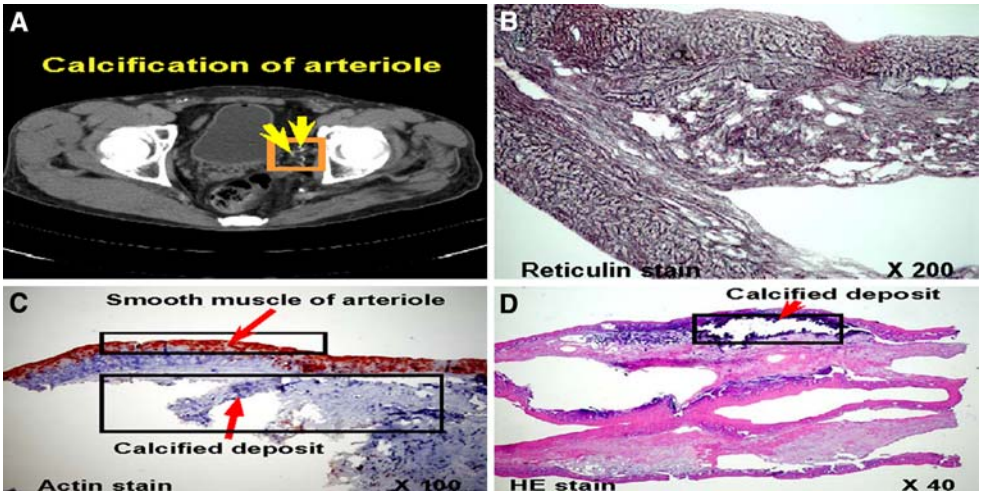

Fig. 1 Computed tomography results revealed a calcific deposit in pelvic cavity of patient (**A**), and different histopathological examinations were carried out to confirm that calcified deposit was obstructed within the superior vesical artery (**B**–**D**)

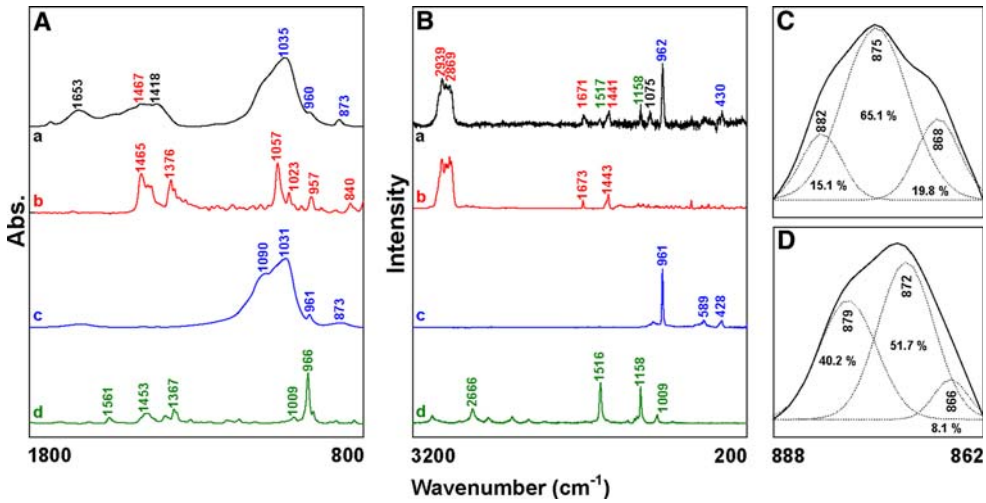

Fig. 2 The FT-IR (**A**) and Raman (**B**) spectra of calcified deposit (*a*), cholesterol (*b*), hydroxyapatite (*c*) and *β*-carotene (*d*), and the curve-fitted IR spectra of hydroxyapatite (**C**) and calcified deposit (**D**)

calcified deposit, which was mainly due to the v_1 phosphate stretching mode of the HA. The main spectral features of cholesterol were located at 1,673 (C=C stretching mode), 1,443 (CH_2/CH_3 bending vibration) and 2,950–2,800 cm^{-1}, which all presented in the Raman spectrum of calcified deposit [9]. Two strong C=C and C–C stretching vibrations at 1,516 and 1,158 cm^{-1} were observed in both Raman spectra of *β*-carotene and calcified deposit [10]. Thus, it is evident that the calcified deposit was major consisted of HA, cholesterol and *β*-carotene. This was also consistent with that of the components in the intact human coronary artery atherosclerotic lesions [11].

Biological mineralization is the sophisticated process for production of the inorganic minerals in living organisms. Several mineralized human tissues such as bone and teeth, are naturally produced to contribute to the human body, but crystal deposition disease is also a type of biomineralization process causing much disorders and symptoms in different human organs. The occurrence of calculi in urinary system is the most common urinary disease. The determination of chemical composition of urinary calculi is important in understanding their etiology and for providing primary preventive medical treatment [8]. To our knowledge, this is the first report to find out the obliteration of superior vesical artery caused by calcified deposit. Moreover, the application of FT-IR and Raman microscopic techniques in the assessments of calcified deposit in superior vesical artery was also initially studied. Three compositions of HA, cholesterol and *β*-carotene were qualitatively identified to construct the composition of calcified deposit in superior vesical artery.

The location of the carbonate ions in biological minerals plays an important role in biomineralization process. This location was easily determined by FT-IR vibrational spectroscopy [12]. In fully mature minerals, the carbonate ions may occupy two anionic sites of the apatite structure:

carbonate may replace either hydroxide site (defined as A-type carbonated apatite) or phosphate site (defined as B-type carbonated apatite) in the crystal lattice of apatites or may be in unstable locations. The IR spectrum reflected the above sites within the spectral region of 860–890 cm^{-1} as follows: a band near at 871 cm^{-1} was due to the B-type carbonated apatite; a band at 878 cm^{-1} was assigned to A-type carbonated apatite and a band at 866 cm^{-1} was due to an unstable carbonate location [6, 7, 13]. Here, three components in the typical IR spectra of HA and calcified deposit in superior vesical artery were quantitatively estimated by a curved-fitting analysis: 882 (15.1%), 875 (65.1%) and 868 (19.8%) cm^{-1} for the HA sample, but 879 (40.2%), 872 (51.7%) and 868 (8.1%) cm^{-1} for the calcified deposit, respectively (Fig. 2C, D).

It has been reported that the relative quantities of A-type and B-type carbonate in the human bone mineral have been shown to vary by age of the individual. An increase of A-type carbonated apatite is found in the old bone, but B-type carbonated apatite is the most abundant species in young bone [13]. Here, the abundant amount of A-type carbonated apatite and lesser amount of the unstable carbonate were obtained in the calcified deposit of superior vesical artery than that of the HA sample, suggesting that the calcified deposit was greatly constructed by the matured crystalline stoichiometric apatite. This strongly implies that the calcified deposit in superior vesical artery was close to a mature mineralized product via a longer progressive calcification process with age. The appearance of IR peak at 1,035 cm^{-1} assigned to the matured crystalline stoichiometric apatite also confirmed this result [7, 14, 15].

In summary, the calcification of superior vesical artery has first been reported. Three predominant compositions of calcified deposit were consisted of hydroxyapatite, cholesterol and β-carotene by using FT-IR and Raman microspectroscopies.

References

1. Lin TL, Wein AJ, Gill HS, Levin RM (2005) Functional effect of chronic ischemia on the rabbit urinary bladder. Neurourol Urodyn 7:1–12
2. Untereiner V, Piot O, Diebold MD, Bouché O, Scaglia E, Manfait M (2009) Optical diagnosis of peritoneal metastases by infrared microscopic imaging. Anal Bioanal Chem 393:1619–1627
3. Petter CH, Heigl N, Rainer M, Bakry R, Pallua J, Bonn GK, Huck CW (2009) Development and application of Fourier-transform infrared chemical imaging of tumour in human tissue. Curr Med Chem 16:318–326
4. Antonakos A, Liarokapis E, Leventouri T (2007) Micro-Raman and FTIR studies of synthetic and natural apatites. Biomaterials 28:3043–3054
5. Carden A, Morris MD (2000) Application of vibrational spectroscopy to the study of mineralized tissues (review). J Biomed Opt 5:259–268
6. Lin SY, Li MJ, Cheng WT (2007) FT-IR and Raman vibrational microspectroscopies used for spectral biodiagnosis of human tissues. Spectroscopy 21:1–30
7. Chen KH, Li MJ, Cheng WT, Balic-Zunic T, Lin SY (2009) Identification of monoclinic calcium pyrophosphate dihydrate and hydroxyapatite in human sclera using Raman microspectroscopy. Int J Exp Pathol 90:74–78
8. Carmona P, Bellanato J, Escolar E (1997) Infrared and Raman spectroscopy of urinary calculi: A review. Biospectroscopy 3:331–346
9. Römer TJ, Brennan JF 3rd, Schut TC, Wolthuis R, van den Hoogen RC, Emeis JJ, van der Laarse A, Bruschke AV, Puppels GJ (1998) Raman spectroscopy for quantifying cholesterol in intact coronary artery wall. Atherosclerosis 141:117–124
10. Lin SY, Chen KH, Cheng WT, Wang SL (2007) Preliminary identification of β-carotene in the vitreous asteroid bodies by micro-Raman spectroscopy and HPLC analysis. Microsc Microanal 13:128–132
11. Buschman HP, Deinum G, Motz JT, Fitzmaurice M, Kramer JR, van der Laarse A, Bruschke AV, Feld MS (2001) Raman microspectroscopy of human coronary atherosclerosis: biochemical assessment of cellular and extracellular morphologic structures in situ. Cardiovasc Pathol 10:69–82
12. Boskey AL, Mendelsohn R (2005) Infrared spectroscopic characterization of mineralized tissues. Vib Spectrosc 38:107–114
13. Rey C, Collins B, Goehl T, Dickson IR, Glimcher MJ (1989) The carbonate environment in bone mineral: a resolution-enhanced Fourier Transform Infrared Spectroscopy Study. Calcif Tissue Int 45:157–164
14. Paschalis EP, DiCarlo E, Betts F, Sherman P, Mendelsohn R, Boskey AL (1996) FTIR microspectroscopic analysis of human osteonal bone. Calcif Tissue Int 59:480–487
15. Faibish D, Gomes A, Boivin G, Binderman I, Boskey A (2005) Infrared imaging of calcified tissue in bone biopsies from adults with osteomalacia. Bone 36:6–12